NANO 3D PRINTING-ENABLED MICROPOST ARRAY GRADIENTS

Aaman Mengis, Riddhi Gopal, Naomi Feldman, Nikita Kedia, David Hesley, Jessica Young, Theodore Fobe, Lucia Fernandez, Christine Anderson and Ryan D. Sochol*
Department of Mechanical Engineering, University of Maryland, College Park, MD, USA

ABSTRACT

Here we introduce a two-photon Direct Laser Writing (DLW) strategy to create arrays of dual-structured microposts that vary in height (and therefore, stiffness) from post-to-post for cell mechanobiological studies. Using the Nanoscribe Professional GT system, we tuned the mechanical stiffness of each arrayed micropost through changes in relative heights of dual-structured posts. ANSYS simulations revealed that the theoretical stiffness of microposts could be modulated in the range of 2 to 250 nN/μm over the length of an array. Experimental results obtained from seeding human umbilical vein endothelial cells (HUVECs) revealed cell-generated traction forces up to 37.1 +/- 7.2 nN. We envision that the ability to measure the traction forces of cells seeded on the presented stiffness gradients will enable researchers to better understand, and subsequently, control cellular behaviors, thereby impacting fields including tissue engineering, biomaterials, and regenerative medicine.

INTRODUCTION

Cellular Durotaxis

One of the goals of cell mechanobiology is to elucidate how cells are influenced by mechanical factors in their surrounding microenvironment. In the past, researchers have focused on investigating the biochemical processes that allow a cell to interact with its environment; however, biomechanical stimuli have also been shown to be critical to cellular function [1,2]. Prior research has shown that external forces, such as substrate-based mechanical cues, influence cellular migration [3]. In a phenomenon known as durotaxis, adherent cells sense and respond to substrates with higher stiffness, causing cells to migrate up higher rigidity gradients [4]. This behavior is postulated to contribute to immune response and wound healing [5-7], epithelial-to-mesenchymal transition [8,9], and cancer metastasis [10-12]. Unfortunately, the fabrication of instructive platforms with which durotaxis-based cellular functions can be probed and/or investigated has remained a critical challenge, particularly due to the difficulties associated with tuning the mechanical stiffness of the substrate with high precision (e.g., < 10 μm) and accuracy [13,14].

Micropost Arrays

The ability to use micropost arrays to quantify cellular traction forces was first demonstrated by the Christopher Chen group. Each array is designed to contain microposts, modeled as mechanical cantilevers, with heights and radii ≤ 10 μm. Cells are seeded on the top of the microposts and image analysis is then conducted to determine the cell-generated traction forces corresponding to the micropost deflection. Previous researchers have manufactured micropost arrays with gradient stiffnesses either through changes in radius or through changes in height. Though these methods effectively changed the stiffness of the microposts, they produced confounding effects upon the cell's migration. Fu et al. revealed that by varying micropost heights (to regulate stiffness), micropost stiffness can also affect stem cell fate decisions [16]. Higher stiffness microposts with increased radius, as demonstrated by Sochol et al. had increases in the ECM-coated attachment area at the top of the post, which could also impact cellular attachments and migration [17]. The method employed by Tan et al. to vary stiffness using height proved to be ineffective due to the inability to include large numbers of microposts heights; this constraint results from the complexity and physical limitations of traditional micropost array fabrication [18]. Recently, researchers have modified micropost stiffness through three different strategies to resolve step gradients in rigidity. One method, as demonstrated by Trichet et al., entails including two sets of microposts corresponding to two distinct radii to resolve a single step change in micropost stiffness [19].

Another approach includes a single step change in micropost height, and thus, micropost stiffness [20]. A

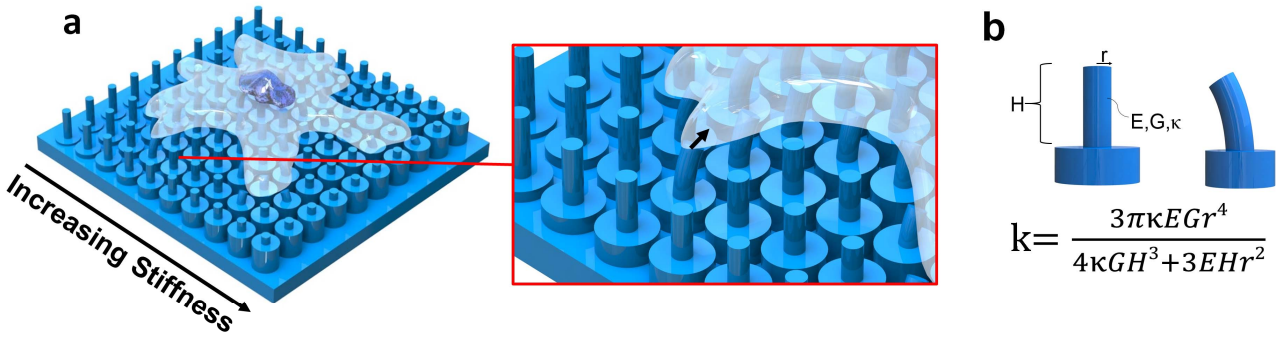

Figure 1: (a) Illustrates micropost arrays manufactured through nano 3D printing to analyze cell migration in response to rigidity. (b) Comparison between bend in the flexible top section of a micropost that is untouched (left) and experiencing cell generated forces (right). Stiffness equation pictured was used to calculate top section heights.

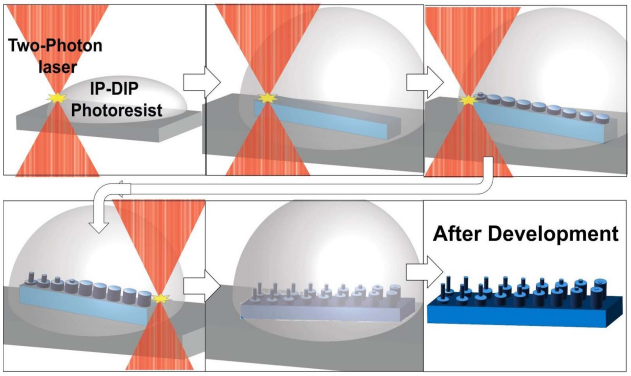

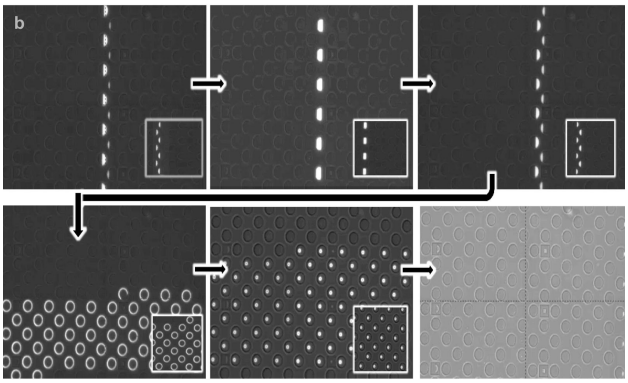

Figure 2: (a) Conceptual illustration of the fabrication of a post array using 3D laser lithography on a nanoscale. The two photon laser polymerizes the photoresist at the depicted focal point to accurately fabricate each layer of the 1x1mm array. (b) Images from a real time video of the nano 3D printer depicting the fabrication of a low gradient micropost array mold.

third concept involves using one set of microposts with a single radius and an adjacent set of dual-structured microposts in which each post includes a bottom section with a large radius and a top section with a radius that matches that of the first set of posts. The benefit of the latter two approaches is that the ECM area on top of each micropost remains constant throughout the step gradient; however, these substrates are especially challenging to construct from a microfabrication standpoint as such geometries requires an additional spin-coating layer, photomask alignment step, and chemical development process [20,21]. Furthermore, achieving continuous gradients in micropost stiffness (with many distinct micropost stiffness magnitudes) via either of the latter two methodologies would be infeasible [20,21]. Our approach in manufacturing micropost arrays with linearly varying stiffness increases the efficiency and reliability of production while also significantly improving the range of gradients possible.

CONCEPT

Here we introduce a 3D printing-based cellular substrate stiffness gradient comprised of high numbers of discrete, microscale stiffness 'steps' while maintaining consistent extracellular matrix (ECM) coverage. We employed a novel DLW-based approach to 3D print moldable structures that enable geometric characteristics of each individual dual-structured micropost to be customized. The microposts are comprised of a bottom post and a top post. The radius of the bottom post (8 μm) and radius of the top post (2 μm) are kept constant, while the ratio of the two heights vary to change stiffness (Figure 1). Proof-of-concept micropost array rigidity gradients were designed with microposts that decreased the height of the top pillar from 9.51μm to 0.891μm, with corresponding changes in stiffness from 2 to 250nN/μm, respectively. These arrays were micromolded with polydimethylsiloxane (PDMS).

FABRICATION

Direct Laser Writing (DLW)

The micropost array molds in this study were fabricated *via* a DLW process using the Nanoscribe GT Professional system. DLW entails using a femtosecond laser to photopolymerize a liquid-phase photoreactive material (*via* multiphoton absorption) at spatially-controlled locations in space, affording feature resolutions in the 100 nm range (Fig. 2). We leveraged these capabilities to create molds from which dual-structured microposts with a flexible top section and a functionally rigid bottom section can be resolved. Over the length of the array, the bottom post height is increased while the top height is decreased (the combined height remains constant) to increase micropost stiffness (k) from post-to-post in a single direction.

Micromolding

From this 3D printed mold, we used the silicone elastomer, polydimethylsiloxane (PDMS) to create multiple micropost arrays used for cell testing. PDMS is used as the substrate material in direct contact with the cells due to its biocompatible nature and flexibility as a deformable material. These micropost arrays were fabricated using standard soft lithography micromolding protocols and a PDMS ratio of 10:1 base to curing agent. The PDMS micropost arrays were stained with fluorescently labeled bovine serum (BSA). After several hours, cells were fixed upon the arrays and stained using 4',6-diamidino-2-phenylindole (DAPI) to visualize the nucleus.

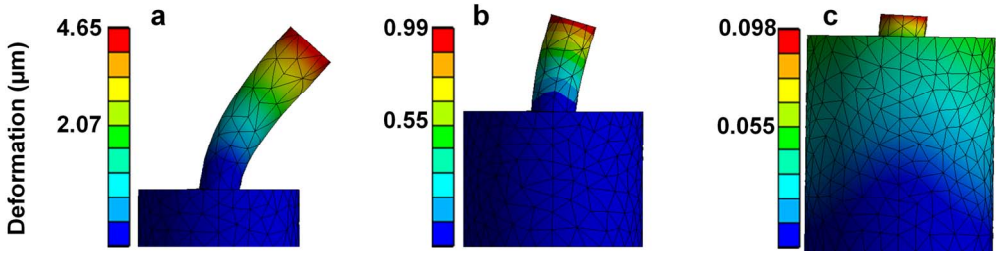

Figure 3: ANSYS deformation simulation of (a) 4.5nN/m, (b) 20nN/m, and (c) 150nN/m stiffness posts due to a 20nN force applied tangentially to the top surface of the microposts

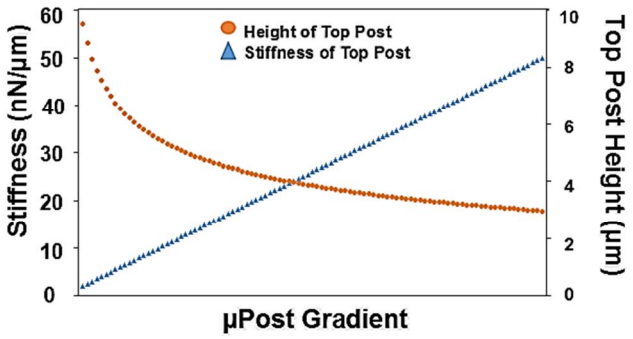

Figure 4: Graph illustrating the linear change in micropost stiffness due to the cubic change in height in the low gradient post.

RESULTS AND DISCUSSION

Theoretical Results

Theoretical stimulations results were performed to investigate the relationship between varying dual-structured micropost geometries and the resulting mechanical stiffness. Examples of stimulation results are presented in Figure 3. As shown, increasing the proportion of the bottom micropost height resulted in a significant decrease in the overall micropost stiffness. While the micropost array stiffness increases linearly to the right, the height decreases to the third power. The theoretical relationship between the stiffness of each post with relation to the height of its top post is presented in Figure 4.

Fabrication Results

The 3D printed micropost molds presented in figure 5a shows the high gradient mold used to create the PDMS micropost arrays. The DLW fabrication process resulted in a high resolution mold; however, resolution was lost between in the PDMS molding process as shown in figure 5b. Several of the microposts within the array had top parts that bent and laid on top of the bottom part of the post. This occurred more often in the higher stiffness microposts. A smaller error within the PDMS formation was the curved tops of each microposts. In the 3D printed mold, each post had 90° corners; however, in the PDMS microposts the tops are rounded.

To improve fabrication results of microposts in further research, we will focus on strengthening the posts. By increasing the top and bottom radius, the microposts will have greater stiffness and decrease the frequency of folded posts in the micropost array. It is important that the columns of microposts with the same stiffness are uniform with no alteration in height. Improving the consistency of our PDMS fabrication will lead to more reliable traction force results.

Cell Results

The cells were imaged using brightfield and fluorescent microscopy as pictured in Figure 6a. The fluorescent images were layered to see the base, the tops and the cells on the array. In the fluorescent images the cells had appeared at both the 558 nm and the 395 nm wavelength. This could be due to the fixing process that permeabilized the membrane which allowed both the EthD-1 and the GFP to enter the cell.

We developed a MATLAB program to quantify the resulting deformation of the micropost from such micrographs. The MATLAB program takes three images of the micropost arrays at three different focuses: one focused on the bases, one focused on the cell, and one focused on the top of the posts. The program then detects the bases and tops of the posts and determines their respective centroids using the Hough transform. A Hough transform is a global method for detecting edges in an image. By searching for certain parameterized functions in a Hough transform of an image, a computer can identify certain features within said image. The differences in the centroids are representative of deformations of the posts resulting from cellular traction forces.

The cellular traction forces are calculated by multiplying the micropost centroid displacement by the micropost-specific stiffness. Figure 6b includes examples of a force field overlaid on fluorescent micrographs of the gradient and cell, with the traction force vectors indicating direction and magnitude of the post deformation. With this process the maximum force calculated was 37.1 +/- 7.62 nN. This measurement, while appropriate for the scale of the experiment is ultimately the result of several erroneous factors. As shown in figure 5b, several post were deformed without the presence of a cell, revealing inadequacies in the design of the post array. In addition, the Hough transforms used to locate the circles may have introduced a significant amount of error to the location of each centroid due to the large range of radii used and the small scale of the circles being detected. This increases the range of the detectible radii, thereby giving a larger margin of error for identifying the correct center of circles. Furthermore, smaller circles are harder to detect using this method. Reducing the range of radii searched for and increasing the overall size of the top circles will aide in better detection of centroids moving forward.

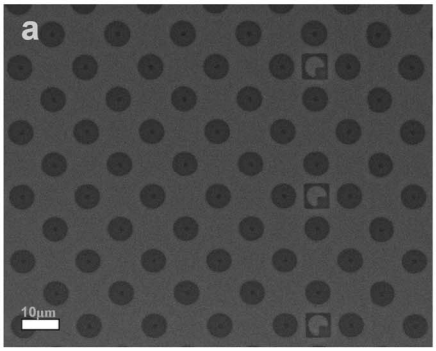

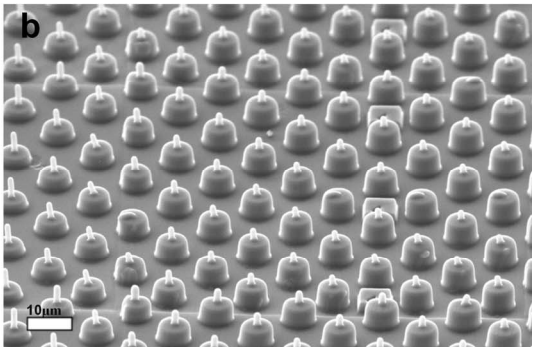

Figure 5: (a) SEM image of nano 3D printed mold used to create PDMS post. (b) SEM image of PDMS microposts made using the 3D printed mold.

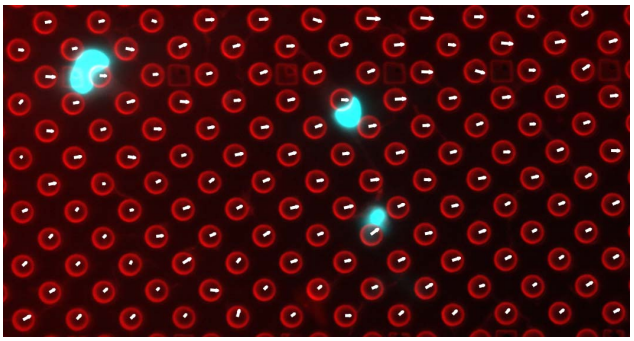

Figure 6: Cells (cyan) on micropost with vectors quantifying direction and relative applied magnitude.

CONCLUSIONS

Using this 3D printing-enabled fabrication methodology, we are able to include high amounts of micropost heights which effectively creates a continuous gradient with constant ECM contact area and is therefore able to accurately measure cell migration solely due to substrate stiffness. We envision that the ability to measure the forces of cells seeded on the presented stiffness gradients will enable researchers to better predict, and subsequently, control cellular behaviors, thereby impacting fields including tissue engineering, biomaterials, and regenerative medicine.

REFERENCES

[1] G. C. Gurtner, S. Werner, Y. Barrandon, and M. T. Longaker, "Wound repair and regeneration," *Nature,* vol. 453, pp. 314-321, 2008.

[2] D. H. Kim, P. K. Wong, J. Park, A. Levchenko, and Y. Sun, "Microengineered Platforms for Cell Mechanobiology," *Annual Review of Biomedical Engineering,* vol. 11, pp. 203-233, 2009.

[3] D. H. Kim, P. K. Wong, J. Park, A. Levchenko, and Y. Sun, "Microengineered platforms for cell mechanobiology," Annual Review of Biomedical Engineering, vol. 11, pp. 203-233, 2009.

[4] Lo, C. M., Wang, H. B., Dembo, M., & Wang, Y. L. Biophys J., "Cell Movement Is Guided By the Rigidity of the Subtrate" 79(1), pp. 144–152, 2000.

[5] D. E. Discher, D. J. Mooney, and P. W. Zandstra, "Growth Factors, Matrices, and Forces Combine and Control Stem Cells," *Science,* vol. 324, pp. 1673-1677, 2009-06-26 00:00:00 2009.

[6] J. I. Lopez, I. Kang, W.-K. You, D. M. McDonald, and V. M. Weaver, "In situ force mapping of mammary gland transformation," *Integrative Biology,* vol. 3, pp. 910-921, 2011.

[7] J. Zhou, H. Y. Kim, and L. A. Davidson, "Actomyosin stiffens the vertebrate embryo during crucial stages of elongation and neural tube closure," *Development,* vol. 136, pp. 677-688, 2009-02-15 00:00:00 2009.

[8] W.-h. Guo, M. T. Frey, N. A. Burnham, and Y.-l. Wang, "Substrate Rigidity Regulates the Formation and Maintenance of Tissues," *Biophysical Journal,* vol. 90, pp. 2213-2220.

[9] J. de Rooij, A. Kerstens, G. Danuser, M. A. Schwartz, and C. M. Waterman-Storer, "Integrin-dependent actomyosin contraction regulates epithelial cell scattering," *The Journal of Cell Biology,* vol. 171, pp. 153-164, October 10, 2005.

[10] M. J. Paszek, N. Zahir, K. R. Johnson, J. N. Lakins, G. I. Rozenberg, A. Gefen, C. A. Reinhart-King, S. S. Margulies, M. Dembo, D. Boettiger, D. A. Hammer, and V. M. Weaver, "Tensional homeostasis and the malignant phenotype," *Cancer Cell,* vol. 8, pp. 241-54, Sep 2005.

[11] M. A. Wozniak, R. Desai, P. A. Solski, C. J. Der, and P. J. Keely, "ROCK-generated contractility regulates breast epithelial cell differentiation in response to the physical properties of a three-dimensional collagen matrix," *J Cell Biol,* vol. 163, pp. 583-95, Nov 10 2003.

[12] T. A. Ulrich, E. M. de Juan Pardo, and S. Kumar, "The mechanical rigidity of the extracellular matrix regulates the structure, motility, and proliferation of glioma cells," *Cancer Res,* vol. 69, pp. 4167-74, 2009.

[13] M. Singh, C. Berkland, and M. S. Detamore, "Strategies and Applications for Incorporating Physical and Chemical Signal Gradients in Tissue Engineering," *Tissue Engineering Part B-Reviews,* vol. 14, pp. 341-366

[14] Sergey V. Plotnikov, Ana M. Pasapera, B. Sabass, and Clare M. Waterman, "Force Fluctuations within Focal Adhesions Mediate ECM-Rigidity Sensing to Guide Directed Cell Migration," *Cell,* vol. 151, pp. 1513-1527.

[15] D. H. Kim, P. K. Wong, J. Park, A. Levchenko, and Y. Sun, "Microengineered Platforms for Cell Mechanobiology," *Annual Review of Biomedical Engineering,* vol. 11, pp. 203-233, 2009.

[16] J. P. Fu, Y. K. Wang, M. T. Yang, R. A. Desai, X. A. Yu, Z. J. Liu, and C. S. Chen, "Mechanical regulation of cell function with geometrically modulated elastomeric substrates," *Nature Methods,* vol. 7, pp. 733, Sep 2010.

[17] Sochol, R. D., Higa, A. T., Janairo, R. R. R., Li, S., & Lin, L. "Unidirectional Mechanical Cellular Stimuli via Micropost Array Gradients" *Soft Matter*, 4606–4609.

[18] Tan, J. L., Tien, J., Pirone, D. M., Gray, D. S., Bhadriraju, K., & Chen, C. S. "Cells lying on a bed of microneedles: An approach to isolate mechanical forces" Proc. Natl. Acad. Sci. U.S.A., vol. 100, 1484–1489, 2003.

[19] L. Trichet, J. Le Digabel, R. J. Hawkins, S. R. K. Vedula, M. Gupta, C. Ribrault, P. Hersen, R. Voituriez, and B. Ladoux, "Evidence of a large-scale mechanosensing mechanism for cellular adaptation to substrate stiffness," *Proceedings of the National Academy of Sciences,* vol. 109, pp. 6933-6938, May 1, 2012 2012.

[20] M. T. Breckenridge, R. A. Desai, M. T. Yang, J. Fu, and C. S. Chen, "Substrates with Engineered Step Changes in Rigidity Induce Traction Force Polarity and Durotaxis," *Cellular and Molecular Bioengineering,* vol. 7, pp. 26-34, 2013.

[21] S. Lee, J. Hong, and J. Lee, "Cell motility regulation on a stepped micro pillar array device (SMPAD) with a discrete stiffness gradient," *Soft Matter,* 2016.

[22] Sniadecki, N. J., Han, S. J., Ting, L. H., & Feghhi, S. "Micropatterning on Micropost Arrays" In *Methods in Cell Biology*, vol. 121, pp. 61–73, 2014.

CONTACT

*A. Mengis, tel: +301-693-7086; amengis@umd.edu